10.51975/25400101.som
Journal of the Nigerian Society of Chemical Engineers, 40(1), 2025

REMOVAL OF LEAD FROM TEXTILE WASTE WATER USING CHITOSAN PRODUCED FROM SNAIL SHELL

Oyedeko K F K., Akinyanju A S., Lasisi-Amokun M K.
Department of Chemical Engineering, Lagos State University, Epe, Nigeria
Department of Chemical Engineering, University of Lagos, Lagos, Nigeria
Email of the Corresponding author: mlasisi@unilag.edu.ng(+234-7055047648)

ABSTRACT
The sorption process of lead (II) ions from textile effluent was investigated using chitosan obtained from a snail shell (SSC). The effects of various experimental parameters on Pb (II) ions adsorption were studied, and optimal conditions were determined. The equilibrium data were analyzed with Langmuir, Freundlich, Temkin, Elovich, Florry Huggins, Jovanovic, Harkin Jura, and Dubinin–Radushkevich (DRK) adsorption models. The high correlation factor of Langmuir isotherm indicates the monolayer coverage of the adsorbent. Freundlich isotherm fitted the adsorption data excellently. The adsorption intensity (n) is 1.68. This means the suitability of the adsorption process. The adsorption process is beneficial when the adsorption intensity is between 1 and 10. Adsorption kinetics data for sorption of Pb^{2+} ion unto chitosan were analyzed using the pseudo-first order, pseudo-second order, and intraparticle diffusion models. The results indicated that the pseudo-second-order model best described the adsorption kinetic data. For the thermodynamic studies, the enthalpy change, ΔH°, and the entropy change, ΔS°, for the adsorption processes are -18.10 kJ/mol and -0.0652 KJ/mol K respectively. The free energy, ΔG° for the process are 2186.39 J/mol, 3071.761 J/mol, 3689.615J/mol, and 4153.032 J/mol at 303K, 313K, and 323K respectively. The thermodynamic parameters showed that the adsorption of lead into SSC was exothermic and non-spontaneous.
***Keywords**: Adsorption, sorption, chitosan, isotherm, kinetic models, intra-particle diffusion.*

1. INTRODUCTION

Water pollution by the discharge of harmful heavy metals has been one of the problems threatening the human health and ecological system. These heavy metals may be released naturally into the environment or through anthropogenic activities like mining and smelting processes, battery and machinery manufacturing, and electroplating plants,(Zhang et al, 2020). Pb(II) is highly toxic and forms complexes in the liver and kidney, resulting in endocrine disorders, and cancer (Ghorbani et al, 2020, Zhu et al, 2021).

Lead is one of the highly toxic heavy metals, that even at a low concentration, can cause serious health hazards to man and aquatic animals. Thus, there is a growing demand for the elimination of toxic metals from polluted areas such as water streams and wastewater to avert their hazardous impacts. (Zhu et al, 2021)

Several methods such as ion exchange (Li. et al, 2021), membrane technology (El-Batouti et al, 2021), precipitation (Qasem et al, 2021), ion exchange (Hussain et, al, 2021), coagulation (Sylwan et al, 2021), co-precipitation (Zhao et al, 2021), electrolysis (Kumar, et al, 2021), and adsorption are being used to remove heavy metals from textile waste. The adsorption technique can be considered useful for removing dissolved heavy metals from liquid wastes. It is also more effective and economical for removing heavy metals from industrial wastewater than other conventional wastewater treatment methods. (Iconaru et al, 2016) The adsorption method is effective in removing from wastewater low concentrations of heavy metal ions and is also used at the industrial level (Khazael, et al 2016 Oliveira, et al 2011). Of all the low-cost adsorbents, chitosan has the highest sorption capacity for several metal ions. (Babel and Kurniawan, 2004; Nomanbhay and Palanisamy, 2005).

The waste derived from snails constitutes environmental challenges after removing the inner part, which greatly benefits human health. Waste generated from the shells of snails is the main precursor for the production of chitosan. Chitosan is one of the low-cost adsorbents with high sorption capacity for metals removal. It is widely used in diverse fields, ranging from waste management to food processing, medicine, and biotechnology (Kalut, 2008). In agriculture, it is used to improve the yield of rice and orchid production (Kim, 2010).

Chitosan is the most common derivative of chitin formed based on chitin partial N-deacetylation through variations of chemical processes with more than one soluble analog. As a result of numerous benefits (non-toxicity, biocompatibility, biodegradability, and non-antigenicity) attributed to chitin and chitosan, they have continued to attract interest worldwide (Daniel and James, 2019). The Chitosan produced through chitin deacetylation is a high molecular weight molecule with a biodegradable polymer and consists of-(14)-2-amino, 2-deoxy- Dglucopyranose (Islam et al., 2017).

Heavy metals discharged into water from various industries are toxic and carcinogenic. They cause severe problems for humans and aquatic ecosystems. Thus, the removal of heavy metals from wastewater is a serious

concern. Both commercial adsorbents and bio-adsorbents are used for the removal of heavy metals from wastewater, with high removal capacity. The challenge in heavy metal removal from wastewater is that it may require large amounts of bio-adsorbents and extra chemicals to maintain a pH that provides suitable conditions for adsorption.

This study aimed to remove Pb^{2+} in the wastewater by adsorption using chitosan. The chitosan used for adsorbent was obtained from a snail shell (SSC).

2. MATERIALS AND METHODS

All the chemical reagents used for this research work were of analytical grade and were supplied by Foray Enterprises Ltd, Lagos State. The raw material used for chitosan production is *Archachatina marginata* (African giant). The reagents are hydrochloric acid and sodium hydroxide. Deionized water used for this research was obtained from the Chemistry Department, University of Lagos, Akoka, Yaba, Lagos.

2.1 PREPARATION OF CHITIN

There are four basic stages involved in the production of chitosan. The stages are Demineralization, deproteinization, depigmentation or decolorization, and deacetylation.

The first stage in Chitosan production is the Demineralization stage. The methods employed for the production of chitin from snail shells were as described by Moosa et al. (2016). 500 g of the sieved sample was weighed and put into a beaker. 2500 ml of 3.2525 M of HCl solution was added (1:5w/v). The mixture was stirred using a griffin shaker at 30 ^{o}C, for 2 hours to avoid effervescence and to remove carbonate and phosphate content. The resulting solution was washed with distilled water and filtered with Whatman filter paper. The residue was scraped into a petri dish and dried in an oven at 105 ^{o}C for 2 hours. In the deproteinization process, the demineralized chitin was soaked in 870 ml of 2.39M of sodium hydroxide (NaOH) solution (1:5w/v). The mixture was stirred and boiled in a water bath at 70 ^{o}C for 2 hours. The resulting solution was filtered with Whatman filter paper and washed with distilled water until the pH of the filtrate was neutral. After washing (as shown in plate 3), the mixture was filtered and the residue was put in an oven at 105 ^{o}C for 2hrs to dry.

2.2 PREPARATION OF CHITOSAN.

The obtained chitin was soaked in 750 mL of 50 wt /wt% NaOH, heated at 85 ^{o}C for 2 hours, 30 mins in a water bath, and cooled for 30 min at room temperature. The mixture was placed on a magnetic stirrer at 30^{o}C for 4 hours. The mixture was washed and the pH of the filtrate was constantly checked until it was neutral. Thereafter, the mixture was filtered using Whatman filter paper to retain the solid matter. The chitosan thus produced was dried in an oven at 105 ^{o}C for 2 hours. This process is known as Deacetylation.

3.0. CHARACTERIZATION OF CHITOSAN

3.1 DEGREE OF DEACETYLATION

The degree of deacetylation (DD) of chitosan is an important parameter to be noted as it affects the solubility, chemical reactivity, and biodegradability of chitosan. DD may range from 30% to 95% (Martino et al., 2005), depending on the available source and procedure.100% DD is very scarcely obtained, with commercial chitosan with various DD in the range of 75-85%. IR technique was used for determining the degree of deacetylation, DD, of chitosan, according to the methods described by (Ghimire et al., 2011): The degree of Deacetylation (DDA) of the refined chitosan from snail shells was calculated using the equation given

$$DD = \left(100 - \frac{A_{1320}}{A_{1420}} \times \frac{1}{0.03133}\right)$$

A_{1320} and A_{1420} are the absorbance values at the wavelengths 1320 and 1420 cm^{-1} respectively. the FTIR analysis of chitosan, the % transmittance of the wavelength 1320 and 1420 cm^{-1} was obtained as 21.5 % and 25.1 % respectively. This was then converted to absorbance [A=2- log (% T), where T is transmittance. The degree of deacetylation of the chitosan sample was obtained to be 64.50%.

3.2 DETERMINATION OF ASH CONTENT

A 2g sample of the sample was weighed into an empty crucible that had previously been heated, cooled, and weighed. This was then kept in the furnace at 600^{o}C for 5 hrs. and later allowed to cool to about 200^{o}C. The crucible was transferred directly into a desiccator to cool to room temperature and weighed immediately. The percentage (%) ash content was calculated as follows (Baby R. et al. 2021)

$$\frac{(\textbf{\textit{Mass of crucible+ash}})-(\textbf{\textit{Mass of empty crucible}})}{\textbf{\textit{Mass of sample used}}} \times \mathbf{100}$$

3.3 DETERMINATION OF MOISTURE CONTENT

A clean crucible was dried in an oven at 105 ^{o}C for 1 hr. cooled in a desiccator, and the mass of the crucible was weighed as W_o. A 5 g sample of the bio sorbent was placed in an oven at 105 ^{o}C for 2hrs, cooled in a desiccator, and weighed. The same procedure was conducted severally until a constant weight was observed. The moisture content of the sample was then calculated (Ajala, LO et al. 2012):

$$\frac{W1-\boldsymbol{W2}}{W1-Wo} \times \mathbf{100}$$

Where the mass of the empty crucible is W_o; that mass of the sample and crucible before heating = W_1 and the mass of the sample and crucible after heating =W_2

3.4 SOLUBILITY

Chitosan dissolution was carried out by dissolving 1 gram of chitosan in 100 ml of 2% acetic acid. The solution is stirred until homogeneous or vortex for 10 seconds. The solution was then centrifuged for 15 minutes and then filtered to get residue on filter paper. The filter paper was

then in the oven at 100-105ºC for 2 hours, the process was repeated until a constant weight was obtained.
Solubility is obtained by inserting into the formula (Shon et al, 2011):

Insolubility (%) = $\frac{Final\ weight\ (g)}{Initial\ weight\ (g)} x\ 100\%$

Solubility (%) = 100% - Insolubility

4.0 BATCH EXPERIMENTS

Batch adsorption was carried out to study how various factors affect the removal of lead (Pb^{+}) from wastewater using locally produced chitosan. The factors considered are pH, adsorbent dosage, contact time, and temperature. 50 mL of known lead solution was put into a 250 mL Erlenmeyer flask at specific conditions. The effects of pH were studied by varying the pH of wastewater using 0.1 M HCl and 0.1 M NaOH. The effect of time was within 130 mins at a fixed mass of 0.1g chitosan and at room temperature of 30 ±1 ºC. Also, a thermodynamics study was carried out with temperature ranges from 30 to 50 ºC at a fixed mass adsorbent of 1g.

4.1 ADSORPTION KINETICS

Adsorption kinetics describes the rate at which solute is adsorbed at the solid–solution interface. This helps to understand the sorption process to design a proper wastewater treatment plant. The kinetic parameters assist in predicting the rate of adsorption and as well as equilibrium time. (Sivarajasekar and Baskat, 2014). Adsorption kinetics is a major issue in the design of a treatment system using adsorbent. Adsorption kinetics provides information that assists industry operators and planners to effectively treat contaminated wastewater. (Olafadehan et. al. 2021). The adsorption kinetics examined in this study as illustrated below.

4.1.1 PSEUDO-FIRST ORDER MODEL

The pseudo-first-order kinetic model, shown in equation 1 below, has been widely used to predict the metal adsorption kinetics. The metal adsorption kinetics following the pseudo-first-order
model is given by (Ho and McKay 2000, Sivaraj 2001)

$$\frac{dq_t}{dt} = K_{e_1}(q_e - q_t) \qquad 1$$

Where

K_{e_1} =equilibrium rate constant of pseudo-first order sorption (min^{-1})

q_t = Integrating equation with the conditions

$q_t = 0 \quad at \quad t = 0$;

$q_t = q_t \quad at \quad t = t$

Integrating and applying the boundary conditions give:

$$In(q_e - q_t) = Inq_e - Ke_1 t$$

Therefore, a straight line should be obtained from the plot of (qe-qt) against t, which is adequate to determine ke_1.

4.1.2 PSEUDO-SECOND ORDER MODEL

The pseudo-second-order kinetic model assumes the adsorption of solutes onto adsorbents follows the second-order mechanism and is expressed as:

$$\frac{dq_t}{dt} = K_{e_2}(q_e - q_t)^2 \qquad 2$$

Integrating and substituting equation conditions.

$q_t = 0\, at\, t = 0;$

$q_t = q_t\, at\, t = t$

$$\frac{1}{(q_e - q_t)} = Ke_2 t + C \qquad 3$$

$q_t = 0 \quad t = 0$

$$C = \frac{1}{q_e}$$

Substituting C into equation 3 above and re-arranging the equation gives

$$\frac{1}{Ke_2 q_e^{\,2}} + \frac{t}{q_e} = \frac{t}{q_t} \qquad 4$$

The plot of $\frac{t}{q_t}$ versus t should give a straight line if pseudo-second-order kinetics are applicable and the values of q_e and k_{e2} can be determined from the slope and intercept respectively.

$h = k_{e2}\, q_e^{\,2}$.

4.1.3 INTRAPARTICLE DIFFUSION (IPD)

One of the most widely used techniques for identifying the mechanism involved in
the adsorption process is an intraparticle diffusion model. The intra-particle diffusion equation is expressed as follows:

$$q_e = k_d t^{1/2} + C \qquad 5$$

where k_d Is the intraparticle diffusion rate constant ($mg/gmin^{1/2}$) and C Is the intercept (mg/g).

The plot of q_t versus $t^{1/2}$ gives a straight line from which the slope of the graph K_d and the intercept C which gives

information about the thickness of the boundary layer can be calculated.

4.1.4 ELOVICH RATE EQUATION

Elovich rate equation is used to describe second-order kinetic, with the assumption that the actual solid surfaces are energetically heterogeneous, (E. Malkoc *et al.*2007). It is given as follows:

$$\frac{dq_t}{dt} = a\exp(-bq_t) \quad 6$$

Integrating and substituting equation conditions and subsequently linearizing the result yields

$$\frac{1}{ab\exp(-bqt)} = t + \frac{1}{ab}.$$

$$bq_t = In(ab) + In(t + t_o)$$

$$q_t = \frac{1}{b}In(ab) + \frac{1}{b}In(t + t_0) \quad 7$$

Where a and b are the parameters of the Elovich rate equation indicating the initial adsorption rate $(mg/g.\min)$ and the desorption constant (g/ mg) respectively. This can further be simplified (Rajeshwari Sivaraj *et al.*, 2010).

$$q_t = \frac{1}{b}In(ab) + \frac{1}{b}Int \quad 8$$

4.1.5 AVRAMI KINETIC MODEL

The Avrami kinetic model assumes arbitrary nucleation locations across the reaction surface of the adsorbent. It evaluates changes in kinetic parameters as a function of reaction time and temperature. The linear form of the expression is given (Ahmad et al., 2014; Yoro et al., 2017):

$$\ln[\ln(\frac{q_m}{q_{m-}q_t})] = n_{av}lnk_{av} + n_{av}\,lnt \quad 9$$

Where K_{Av} is the Avrami adsorption kinetic constant and n_{Av} is another constant, which is related to the adsorption mechanism changes. The slopes and intersections values of this equation provide the n_{Av} and lnK_{Av} values, respectively.

4.2 THERMODYNAMIC STUDY:

For the determination of thermodynamic parameters, the following were used:

$$K_c = \frac{C_{Ads}}{C_e} \quad 10$$

$$\ln K_e = \frac{\Delta S^0}{R} - \frac{\Delta H^0}{RT} \quad 11$$

$$\Delta G^o = \Delta H^o - T\Delta S^0 \quad 12$$

where Kc: Equilibrium constant Cad: Adsorbed heavy metals concentration

Ce: Equilibrium concentration of metal in solution (mg L^{-1})

G: Change in standard Gibbs free energy (kJ mol^{-1})

H : Change in enthalpy (kJ mol^{-1})

S: Change in entropy (J mol^{-1} K^{-1})

T: Temperature

4.3 ADSORPTION ISOTHERMS

The Freundlich, Langmuir, Temkin, Jovanovic, Harkins-Jura, Flory-Huggins, and Dubinin-Radushkevich isotherms were used to investigate sorption processes. They are expressed in Eq. (13) to Eq. (19) as follows:

A linear form of the Freundlich expression is:

$$Log\,q_e = LogK_f + \frac{1}{n}LogC_e \quad 13$$

The linear form of Langmuir Isotherm is given as:

$$\frac{C_e}{q_e} = \frac{1}{KQ_m} + \frac{C_e}{Q_m} \quad 14$$

The linearized Dubinin-Radushkevich Isotherm is expressed as:

$$lnq_e = lnq_s - \beta\varepsilon^2 \quad 15$$

The linearized Temkin Isotherm is expressed as:

$$q_e = B\ln A_T + B\,lnC_e \quad 16$$

A_T = Temkin isotherm equilibrium binding constant (L/g)

b_T = Temkin isotherm constant

R = universal gas constant (8.314 J/mol/K)

T = Temperature at 298 K

B = constant related to heat of sorption (J/mol)

The plot of q_e against lnC_e is required to fit the model (Rajeshwari Sivaraj et al., 2010)

The linear form of Harkins- Jura Adsorption Isotherm is given as:

$$\frac{1}{q_e^{\,2}} = \left(\frac{B}{A}\right) - \left[\left(\frac{1}{A}\right)(Log\,C_e)\right] \quad 17$$

C_e Is the equilibrium concentration (mg/l) and q_e Is the amount adsorbed onto the adsorbent (mg/g)

Where A and B are constants. The plot of 1/qe against Log Ce gives the required fit for the model (Rajeshwari Sivaraj*et al.*, 2010).

The linearized form Jovanovic Isotherm is expressed as:

$$\ln q_e = lnq_{max} - K_J C_e \quad 18$$

The linearized form of Flory- Huggins Isotherm is expressed as:

$$\ln\frac{\theta}{C_o} = logK_{FH} + \alpha_{FH} ln(1-\theta) \quad 19$$

where: $\theta = 1 - \frac{C_e}{C_o}$

The values of K_{FH} and α_{FH} are determined from the intercept and the slope of the plot of $\ln\frac{\theta}{C_o}$ versus ln(1-θ) (Hossain et al, 2016)

5. RESULTS AND DISCUSSION

The experimental data were fitted into different adsorption isotherms: Langmuir, Freundlich, Temkin isotherm, Toth adsorption isotherm, Dubinin-Radushkevich (DRK), Harkins-Jura Adsorption Isotherm, Jovanovic Isotherm, and Flory-Huggins adsorption isotherm. The linear plot of Ce/qe versus Ce suggests the applicability of the Langmuir isotherm (Fig. 1 a) The maximum monolayer coverage (Q_m) from the Langmuir isotherm model was found to be 50.51mg/g, K_L (Langmuir isotherm constant) is 0.00374L/mg, R_L (the separation factor) is 0.217 indicating that the equilibrium sorption was favorable. The coefficient of correlation for Freundlich Isotherm was 0.991. (Fig 1 b). The values K_f and n are constants that show factors affecting the adsorption capacity and the intensity of adsorption. The intensity of adsorption is a suggestion for the bond energies between Pb^{2+} and chitosan. The value of 1.68 for the adsorption intensity showed that the adsorption is more favorable. The heat of the sorption process was estimated from the Temkin isotherm model (Fig. 1 e) to be 9.92 J/mol and the mean free energy was determined from DRK isotherm (Fig. 1g) as 50 KJ/mol. This shows that the adsorption experiment followed a physical process. The Coefficient of correlation, R^2 values were used for fitting the experimental data to these isotherms. As shown in Fig 1, all eight (8) isotherms fitted to the experimental data. Table 1 shows isotherm parameters and their correlation coefficients

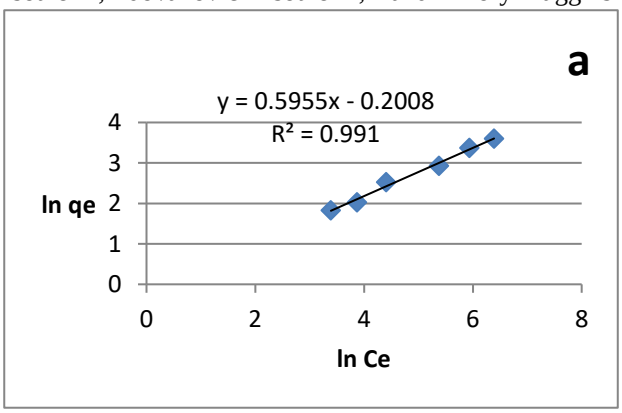

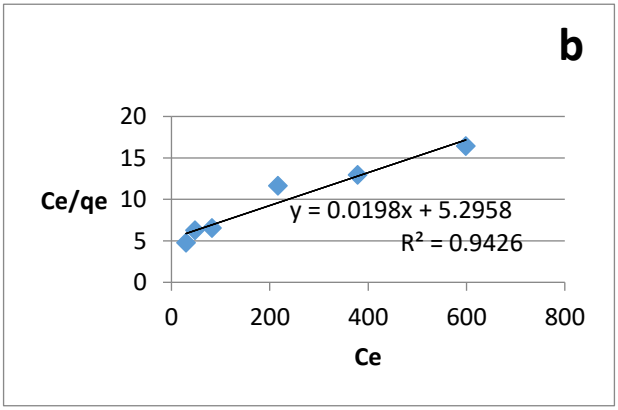

.

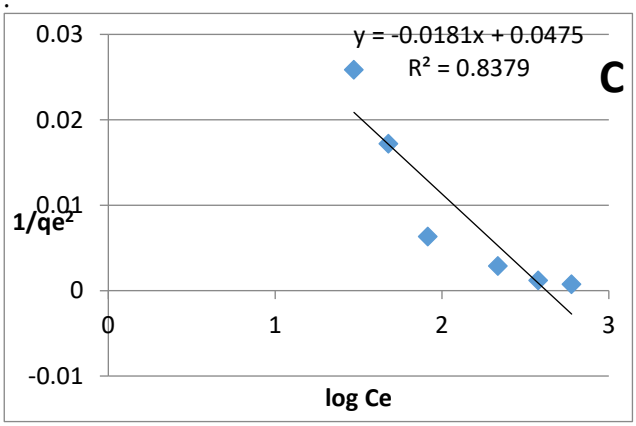

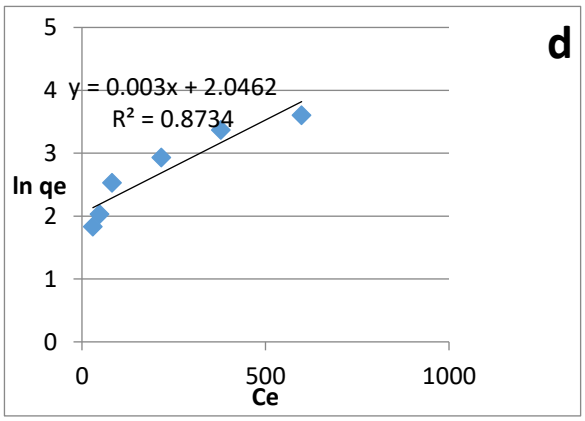

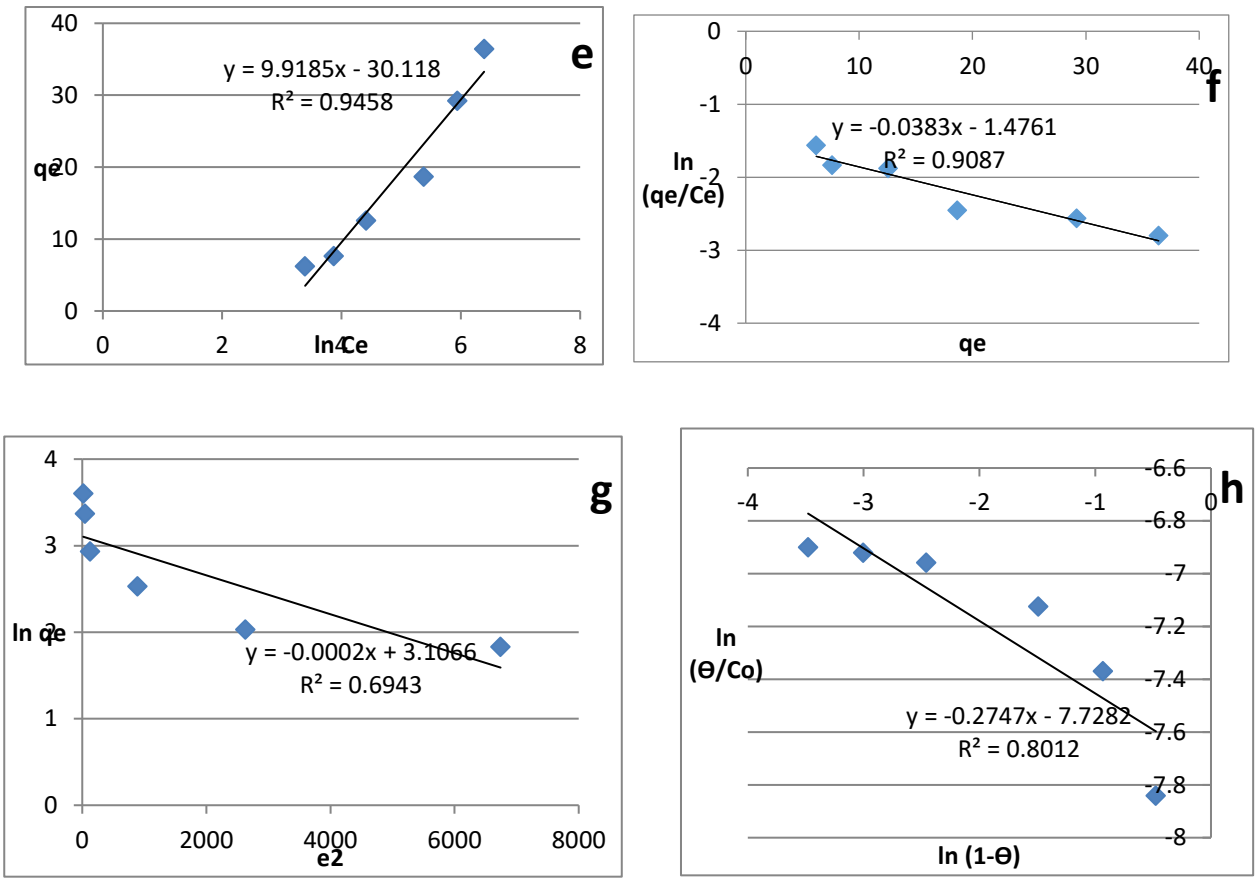

Fig 1(a) Freundlich adsorption Isotherm (b) Langmuir adsorption Isotherm (c) Harkin-Jura adsorption Isotherm (d) Jovanovic adsorption Isotherm (e) Temkin adsorption Isotherm (f) Elovich adsorption Isotherm (g) Dubinin- Radushkevich adsor(DRK) Isotherm (h) Florry- Hugguins adsorption Isotherm

Table 1: Isotherm Constants for Pb2+ ions into Chitosan.

Isotherm Model	Isotherm parameters	Coefficient of Correlation (R^2)
Langmuir	Qm = 50.51(mg/g) K_L = 0.00374 (L/mg) R_L = 0.217	0.943
Freundlich	1/n =0.596 n =1.68 K_f = 0.818 (mg/g)	0.991
Harkin -Jura	B =2.74 A= 63.69	0.816
Jovanovic	K_J = 0.873 q_{max} = 0.774 (mg/g)	0.873
Temkin	A_T = 0.048 (L/mg) B_T = 249.79 B = 9.92 (J/mol	0.946
Elovich	K_e = 0.945 q_m = 26.11	0.909
DRK	Q_m =22.34 β = 0.0002 E = 50 (KJ/mol)	0.694
Florry-Hugguins	α_{FH} = 0.275 K_{FH} =0.531	0.801

Kinetics of Adsorption of Pb^{2+} unto SSC

The kinetics of lead (II) ions adsorption unto chitosan was analyzed using pseudo-first order, pseudo-second order, Elovich, Fractional Power model, Bangham's model (pore diffusion model), Avrami kinetic model, and Intraparticle diffusion models. The kinetic modeling of Pb (II) ions adsorption showed that the pseudo-second-order kinetic model gave the best fit among the investigated kinetic models.

As shown in Fig 2, the experimental kinetic data fitted perfectly into all the kinetic models. The R^2 values of all the models are close to unity. The linear plot of the intraparticle diffusion model (Fig.2) did not pass through the origin. This showed that the Intraparticle kinetic model was not the rate-controlling step in the adsorption of Pb^{2+} into SSC. It means that there is some degree of boundary layer diffusion. The sorption can be approximated more by the pseudo-second-order kinetic model than by the first order kinetic model.

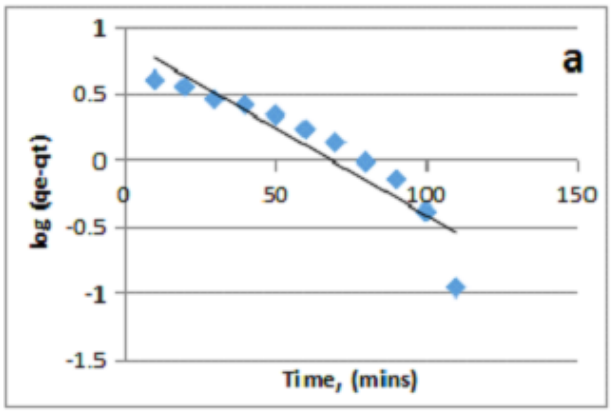

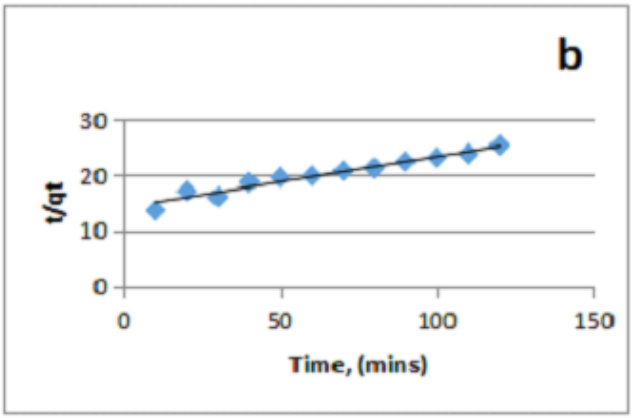

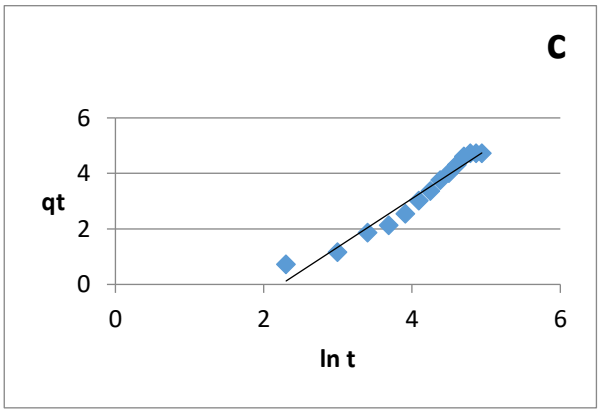

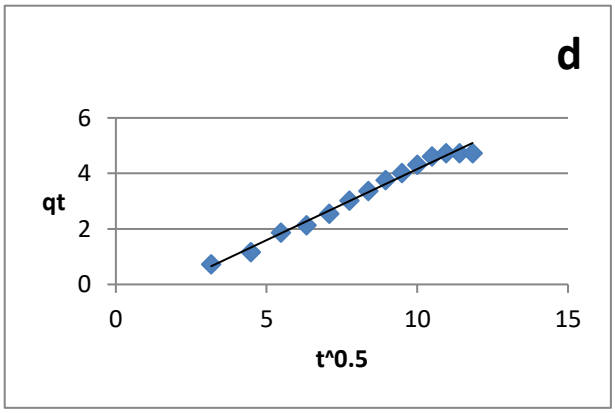

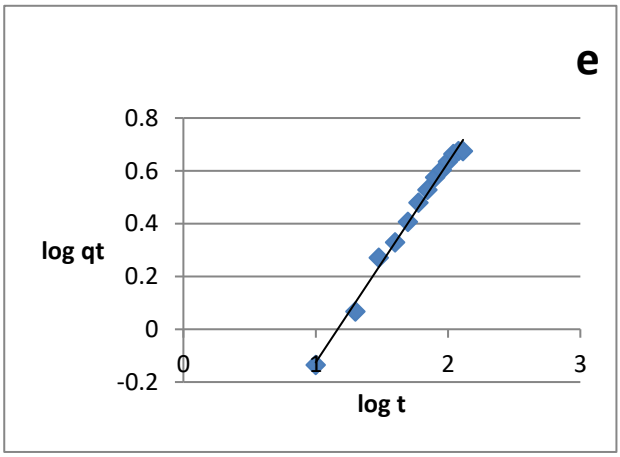

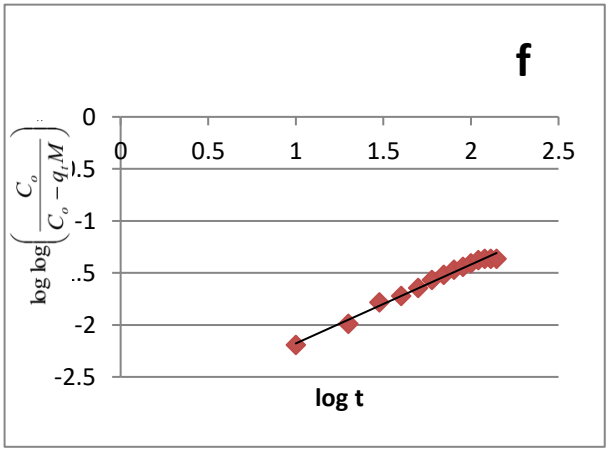

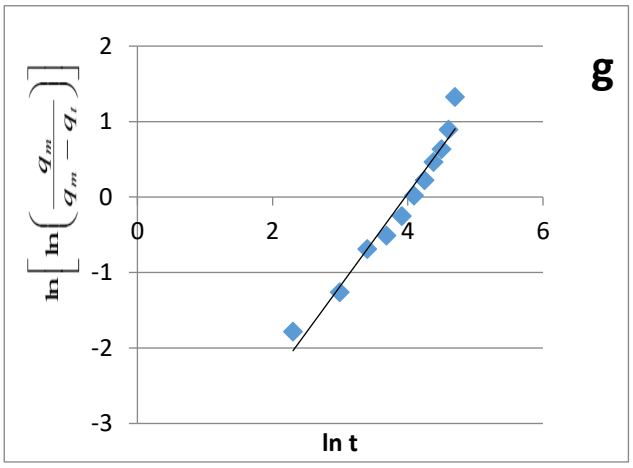

Fig 2 (a) Pseudo-first order kinetic (b) Pseudo-second order kinetic (c) Elovich plot (d) Intraparticle diffusion plot (e) Fractional power model plot (f) Bangham's model plot (g) Avrami kinetic model plot

Table 2: Parameters in the linearized kinetic models for the adsorption of Pb^{2+} on chitosan.

Kinetic Model	Parameters	Values
	H (g/mg min)	0.0706
Pseudo-Second order	K_2 (g/mg min)	5.961×10^{-4}
	qe (mg/g)	10.88
	R^2	0.9531
Pseudo-First order	K_1 (min^{-1})	0.032
	qe(mg/g)	7.909
	R^2	0.8649
Intraparticle	K_d ($mg/gmin^{1/2}$)	0.5122
	C (mg/g)	0.964
	R^2	0.9865
Elovich	a (mg/g min)	0.1877
	b (g/mg)	0.5721
	R^2	0.9584
Fractional Power model	v	0.757
	K	0.131
	R^2	0.9927
Bangham	K_B	0.266
	b	0.759
	R^2	0.9893
Avrami	K_{AV}	0.0190
	n_{AV}	1.226
	R^2	0.9581

Proximate Analysis of Chitosan

The proximate analysis of SSC is shown in Table 3 below. The solubility is one of the standards used to determine the quality of chitosan. The higher the solubility, the better the quality of the chitosan produced. The SSC has a solubility of 94.63%. The solubility of chitosan was examined using water and acetic acid. It was found that chitosan was no soluble in water but partially soluble in acetic acid. The Moisture content and ash content of chitosan were found to be 3.24 % and 1.21% respectively. The protein of the chitosan was 3.11%.

Table 3: Results of Proximate Analysis of Chitosan

Parameters	Chitosan
Solubility (%)	94.63
Moisture Content (%)	3.24
Ash content (%)	1.21
Protein (%)	3.11

Scanning Electronic Microscopy

The SEM images, in Fig 3 (a) and 3 (b) revealed the surface morphology of chitosan from snail shells. The morphology of the adsorbent was observed to be rough and possessed irregular shape particles capable of adsorption of metals from solution. It was observed that the SSC biopolymer possesses porous and fibril structures.

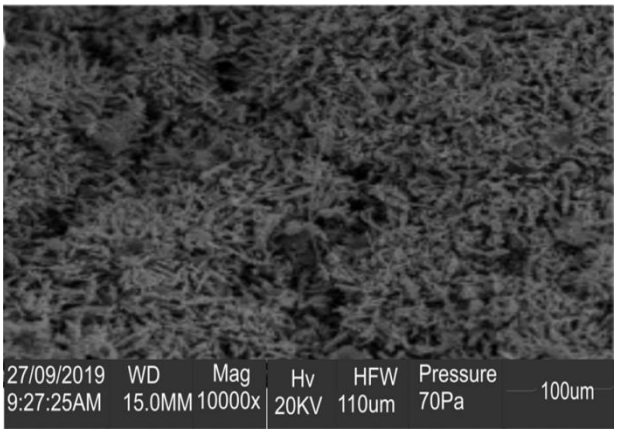

Fig 3 a: SEM Image of Chitosan at X10000

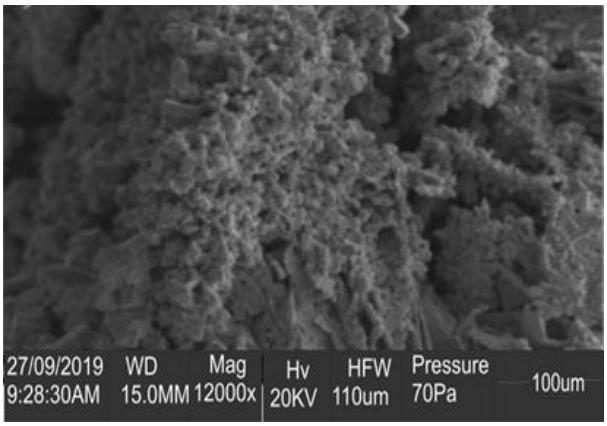

Fig 3 b: SEM Image of Chitosan at X12000

EDS Analysis of Chitosan

The result of Energy Dispersive X-ray Spectroscopy (EDS) shows the elements present in the SSC. Oxygen, Carbon, Magnesium, Calcium, and phosphorus are present in the chitosan sample as shown in Fig 4 below. Oxygen has the highest peak in the EDS spectrum followed by Carbon and calcium respectively. The EDS compositional analysis results obtained on the spectrum of the extracted chitosan from snail shells confirm a weight percent of Oxygen (45.5wt %), Carbon (25.2 wt. %), Magnesium (7.0 wt. %), Calcium (15.7 wt. %) and Phosphorus (1.2 wt. %).

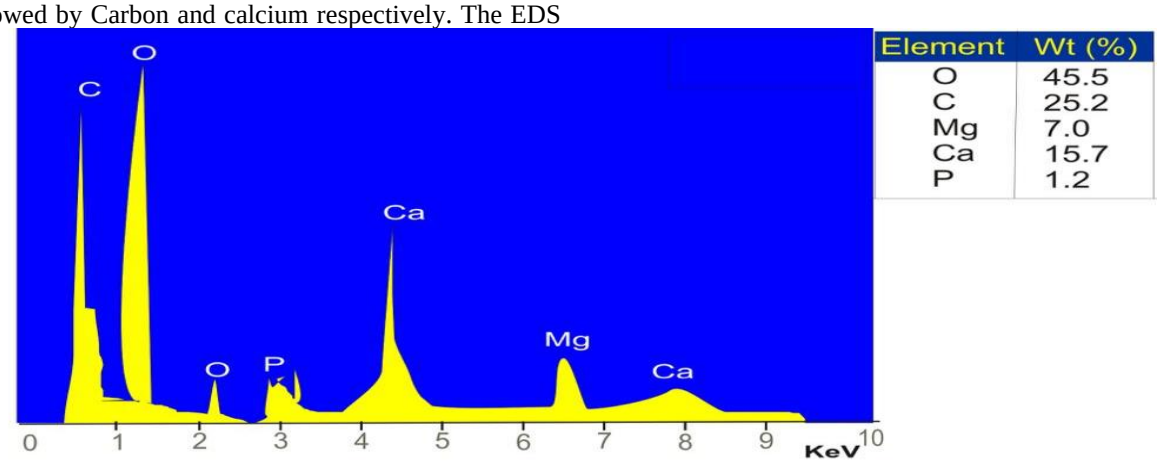

Fig 4: EDS spectra of Chitosan.

Fourier-Transform Infrared (FTIR) Analysis

The FTIR analysis of the adsorbent was determined using a Thermo Scientific Spectrometer. The corresponding spectra of the chitosan showed the wavelengths in the range 4000 to 350 cm^{-1} of the different functional groups in the samples which were identified by comparison with those in the library. As shown in Table 4, The distinct band at 3445cm^{-1} could be attributed to the stretching of $-NH_2$ and -OH present in primary amines and pyranose ring respectively. The band at 2927.76 cm^{-1} could be attributed to $-CH_2$ in the $-CH_2OH$ group, while the observed peak at 1631.73 cm-1 was assigned to -C=O in the $-NHCOCH_3$ group (amide I band). The characteristic band at 1056.00cm^{-1} was assigned to -C-O in the -OH group. Also, the band at 685.36 cm^{-1} was attributed to NH out of the plane. The agreement between the characteristic band of standard chitosan and the chitosan used in this study confirmed the production of chitosan from snail shells.

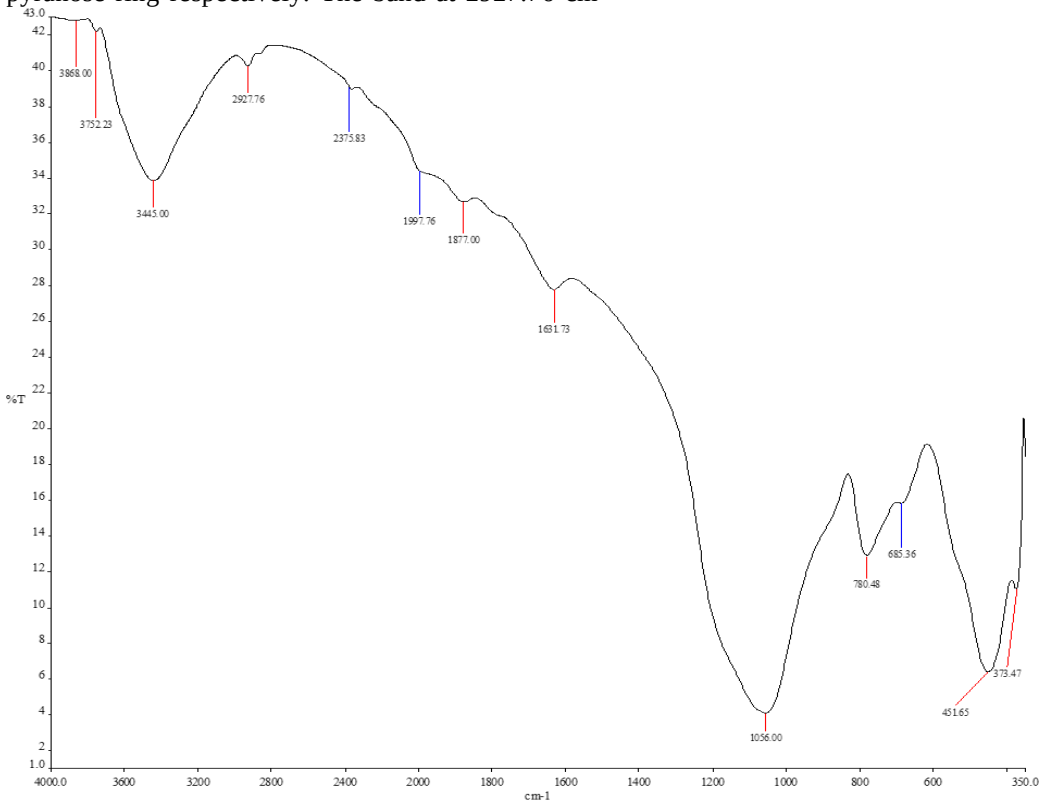

Fig. 5: FTIR Spectra of Chitosan

Table 4: Comparison of FTIR spectrum with standard spectra from Sigma Aldrich

Wavelength			**Functional groups**
Experimental cm^{-1}	Sigma Aldrich Standard cm-1	% error	
3445.00	3422	±0.67	υ(NH2) associated with primary amines and υ (OH) associated with pyranose ring
2927.76	2923	±0.163	υ (CH2) in CH2OH group
1631.73	1655	± 1.41	υ (C=O) in NHCOCH3 group (amide I band)
1562.01	1554	± 0.51	υ (NH2) in NHCOCH3 group (amide II band)
1056.00	1073	±1.58	υ (C–O) in secondary OH group
685.36	662	±3.53	δ (NH) out of the plane

Thermodynamic Study

The thermodynamic study gives an insight into the nature of the adsorption process. As shown in Table 5, the increase in the values of $\Delta G°$ with an increase in temperature indicates that the adsorption process is less favorable at high temperatures. The negative value of $\Delta H°$ means that the adsorption process is exothermic. The small negative value of enthalpy showed that the adsorption process is physical. The enthalpy change, $\Delta H°$, and the entropy change, $\Delta S°$, for the adsorption process are -21.384 kJ/mol and 75.44 J/mol K respectively. The positive value of entropy ($\Delta S°$) showed an increased randomness of the adsorption process.

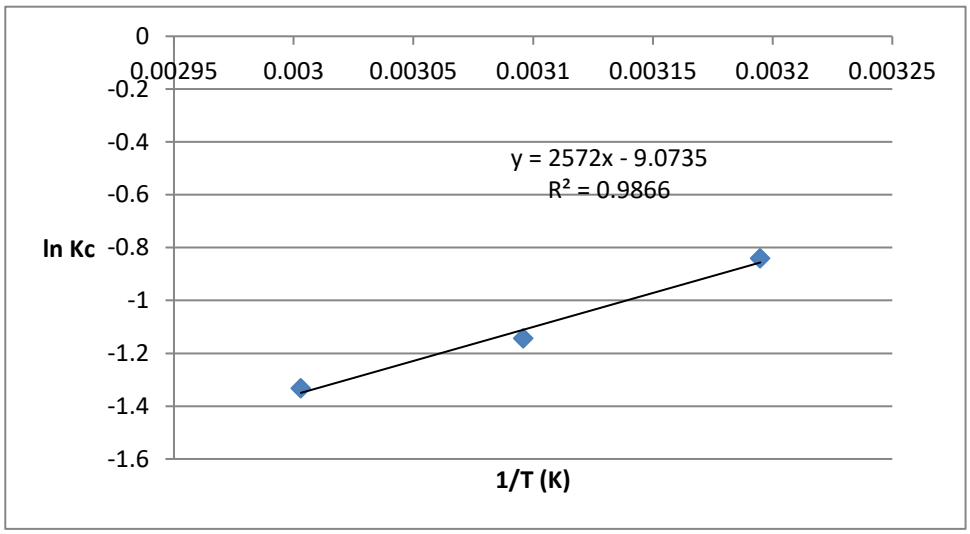

Fig 6: Plot of ln K_c versus 1/T

Table: 5 Thermodynamic parameters for adsorption of lead onto chitosan

Temperature (K)	ΔG (J/mol)	ΔS°(J/mol.K)	ΔH°(KJ/mol)
313	2186.39	**75.44**	-21.384
323	3071.761		
333	3689.615		

6.0 CONCLUSION

The ability of chitosan produced from snail shells as a natural adsorbent to remove Pb^{2+} ions from textile wastewater was investigated in this work. The results showed that SSC is a good adsorbent for the removal of lead Pb (II) from wastewater. It was also observed that the removal of Pb^{2+} increases slightly as the temperature increases. The adsorption Isotherms fitted the adsorption data of Pb^{2+} into SSC.

Kinetic parameters were analyzed using the Pseudo-first order, Pseudo-second order, Intraparticle diffusion, Elovich, Fractional power, Bangham and Avrami model. All the kinetic models excellently fitted the adsorption data Pb^{2+} into chitosan. Kinetic studies showed that the adsorption of Pb^{2+} ions into SSC followed Elovich kinetic model. Intra particle diffusion model was used to determine the adsorption mechanism. However, Intraparticle diffusion was not the rate-determining step because the plot of q_t against $t^{0.5}$ did not pass through the origin. This showed that there was some degree of boundary layer diffusion.

It can be concluded that chitosan from snail shells (SSC) offers an effective and efficient means of removing Pb^{2+} from wastewater.

ACKNOWLEDGMENTS

The author appreciates the support and materials provided by the Department of Chemical Engineering, Lagos State University Epe Campus and University of Lagos, Akoka, Yaba, Lagos, Nigeria, and the assistance of Engr. Amokun Mosunmola Khadijat during manuscript preparation.

REFERENCES

Ahmad MA, Puad NAA, Bello OS (2014). Kinetic, equilibrium, and thermodynamic studies of synthetic dye removal using pomegranate peel-activated carbon prepared by microwave-induced KOH activation. Water Resources and Industry 6:18-35

Ajala, LO, Ali EE, (2012), Preparation and Characterization of groundnut shell-based activated charcoal. J. Appl. Sci Environ Manag. 24(12):2139-16

Babel S, Kumiawan TA (2004). Cr (VI) removal from synthetic wastewater using coconut shell charcoal and commercial activated carbon modified with oxidizing agent and/or chitosan.Chemosphere 54 (7): 951-967

Baby R, Hussein MZ, Zainal Z. ((2021) Functional activated carbon derived from palm kernel shells for the treatment of stimulated heavy metal-contaminated water. Nanometer.;11, 3133.

Daniel T Oyekunle, James A. Omoleye (2019). Effect of particle sizes on the kinetics of demineralization of snail shell for chitin synthesis using acetic acid. Heliyon 5(11):e02828.

El-Batouti, M.; Al-Harby, N. F.; Elewa, M. M. (2021) A. Review on Promising Membrane Technology Approaches for Heavy Metal Removal from Water and Wastewater to Solve Water Crisis. Water, 13, 3241–3262. DOI: 10.3390/w13223241.

Ghimire, S., Neupane, B., Pokhrel, S., Le, H. H., Lebek, W., Heinrich, G., Adhikari, R. (2011). "Conversion of chitin isolated from fresh-water prawns to chitosan and its characterization". Polymers Research Journal, 11(1), 1 15.

Ghorbani M., O. Seyedin, M. Agha Mohammad Hassan, (2020) Adsorptive removal of lead (II) ion from water and wastewater media using carbon-based nanomaterials as unique sorbents: a review, J. Environ. Manage., 109814, https://doi.org/10.1016/j.jenvman.2019.109814.

Hossain, M., Hossain, M., and Hassan, T. (2016). "Equilibrium, Thermodynamic and Mechanism Studies of Malachite". International Letters of Chemistry, Physics Astronomy, 64, 77-88.

Ho YS, Mckay G (2000). The kinetics of sorption of divalent metal ions onto sphagnum moss peat. Water Research 34(3):735-742.

Hussain, S. T.; Ali, S. A. K. (2021) Removal of Heavy Metal by Ion Exchange Using Bentonite Clay. J. Ecol. Eng, 22, 104–111. DOI: 10.12911/22998993/128865.

Iconaru, S. L.; Gu_egan, R.; Popa, C. L.; Motelica-Heino, M.;Ciobanu, C. S.; Predoi, D. Magnetite (Fe3O4) (2016) Nanoparticles as Adsorbents for as and Cu Removal. Appl. Clay Sci., 134,128–135. DOI: 10.1016/j.clay.2016.08.019

Islam S, Bhuiyan MAR, Islam MN (2017). Chitin and Chitosan: Structure, Properties and Applications in Biomedical Engineering. Journal of Polymers and the Environment 25(3):854-866.

Kalut, S.A. (2008) 'Enhancement of Degree of Deacetylation of Chitin in Chitosan Production', pp. 5-31.

Khazael, M., S. Nasseri, M.R. Ganjali, M. Khoobi and R. Nablzadeh et al., (2016). Response Surface Modeling of Lead (II) removal by grapheme oxide- Fe3O4 nanocomposite using Central composite design. J. Environ. Health Sci. Eng., Vol.14. 10.1186/s 40201-016-0243-1.

Khora, E. and Limb, L.Y. (2003) 'Implantable applications of chitin and chitosan', *Biomaterials*, pp. 2339-2349.

Kim, S.K. (2010) *Chitin, Chitosan, Oligosaccharides and Their Derivatives.*, New York: CRC Press.

Kumar, J.; Joshi, H.; Malyan, S. K. (2022) Removal of Copper, Nickel, and Zinc Ions from an Aqueous through Electrochemical and Nanofiltration Membrane Processes. Appl. Sci, 12, 1–15.

Li, M.; Hu, K.; Wang, J.9 (2021) Study on Optimal Conditions of Flocculation in Deinking Wastewater Treatment. J. Eng. Appl. Sci.35, 1–14.

Malkoc E, Nuhoglu Y (2007) Potential of tea factory waste for chromium (VI) removal from aqueous solutions: thermodynamic and kinetic studies. Sep Purif Technol 54:291–298

Moosa, A., Ridha, A., and Kadhim, N. (2016). Use of Biocomposite Adsorbents for the Removal of Methylene Blue Dye from Aqueous Solution. American Journal of Materials Science,6(5), 135-146.

Mujianto. (2012). Sintesis dan Modifikasi Kitosan dari Limbah Kulit Udang Untuk Aplikasi Enhanced Oil Recovery (Synthesis and Modification of Chitosan from Shrimp Shell Waste for Enhanced Oil Recovery Applications). Institut Teknologi Bandung (Bandung Institute of Technology

Nomanbhay S. M, Palanisamy K.; (2005) Removal of heavy metal from industrial Wastewater using chitosan coated oil palm shell charcoal. Electronic Journal of Biotechnology 8, pp.43-53.

Olafadehan OA, Amoo KO, Ajayi TO, Bello VE (2021). Extraction and characterization of chitin and chitosan from Callinectes amnicola and Penaeus notialis shell wastes. Journal of Chemical Engineering and Material Science 12(1):1-30.

Oliveira, E.A., S.F. Montanher and M.C. Rollemberg, (2011). Removal of textile dyes by sorption on low-cost sorbents. A case study: Sorption of reactive dyes onto Luffa cylibdrica. Desalin. Water Treat., 25: 54-64

Qasem, N. A. A.; Mohammed, R. H.; Lawal, D. U. (2021) Removal of Heavy Metal Ions from Wastewater: A Comprehensive and Critical Review. Npj Clean Water, 4, 1–15. DOI: 10.1038/ s41545-021-00127-0.

Rajeshwari S., Venckatesh.R and G.Sangeetha, (2010). "Activated Carbon Prepared from Eichornia Crassipes as an Adsorbent for the Removal of Dyes from Aqueous Solution". *International Journal of Engineering Science and Technology*, Vol.,2 (6), pp 2418-2427.

Shon. (2011). Effect of processing conditions on functional properties of collagen powder from skate (Raja kenojei) skins. Food Science and Biotechnology. 20(1):99-106.

Sivarajasekar N, Baskar R (2014). Adsorption of basic red onto activated carbon derived from immature cotton seeds: isotherm studies and error analysis. Desalination and Water Treatment 52(40- 42):7743-7765

Zhang Y, Y. Chen, W. Kang, H. Han, H. Song, C. Zhang, H. Wang, X. Yang, X. Gong, C. Zhai, (2020) Excellent adsorption of Zn (II) using NaP zeolite adsorbent synthesized from coal fly ash via stage treatment, J. Clean. Prod., 120736, https://doi.org/10.1016/j.jclepro.2020.120736

Zhao, Q.; Xu, T.; Song, X.; Nie, S.; Choi, S. E.; Chuanling, S. I. (2021) Preparation and Application in Water Treatment of Magnetic Biochar. Front. Bioeng. Biotechnol, 9, 2296–4185.

ylwan, I.; Thorin, E. (2021) Removal of Heavy Metals during Primary Treatment of Municipal Wastewater and Possibilities of Enhanced Removal: A Review. Water, 13, 1121. DOI: 10. 3390/w13081121.

Yoro KO, Singo M, Mulopo JL, Daramola MO (2017). Modelling and experimental study of the CO_2 capture. Energy Procedia 114:1643- 1664.

Zhu J, Z. Huang, F. Yang, M. Zhu, J. Cao, J. Chen, Y. Lin, S. Guo, J. Li, Z. Liu, (2021) Cadmium disturbs epigenetic modification and induces DNA damage in mouse preimplantation embryos, Ecotoxicol. Environ. Saf, 306, https://doi.org/10.1016/j.ecoenv.2021.112306.